NOTES AND CORRESPONDENCE

On the Deformation Term in the Quasigeostrophic Omega Equation

JONATHAN E. MARTIN

Department of Atmospheric and Oceanic Sciences, University of Wisconsin—Madison, Madison, Wisconsin

30 July 1997 and 14 October 1997

ABSTRACT

It is a common diagnostic, synoptic practice to consider the Trenberth–Sutcliffe approximation to the quasigeostrophic (QG) omega equation, which relates upward vertical motion to regions of cyclonic vorticity advection by the thermal wind. Use of this approximate form of the QG omega equation requires the neglect of the so-called deformation term, which is often described as important only in frontal regions. Here, an alternative expression for the deformation term is derived that clearly illustrates its relationship to the mathematical forcing function in the **Q**-vector form of the QG omega equation.

The magnitude of the deformation term in the middle troposphere is traced throughout the life cycle of a typical midlatitude cyclone. It is found that this term is generally small at midlevels in the early stages of the cyclone life cycle. As the cyclone approaches and passes its mature stage, however, the deformation term exerts a comparable, locally predominant influence on the total QG forcing for vertical motion. Particularly interesting is the large magnitude this term acquires in the axis of high potential temperature, characteristic of a post–mature stage cyclone's horizontal thermal structure. The large magnitude of the deformation term in such regions demonstrates that there are nonfrontal, midtropospheric regions within cyclones in which the deformation term may not be small.

1. Introduction

In the quasigeostrophic system of equations, diagnosis of the approximate vertical motion from the instantaneous distribution of geopotential height ϕ and temperature T is made possible through use of the quasigeostrophic omega equation (Sutcliffe 1947; Wiin-Nielsen 1959; Trenberth 1978). The conventional, adiabatic form of this equation is given by (Holton 1992)

$$\left(\sigma\nabla^2 + f_o^2\frac{\partial^2}{\partial p^2}\right)\omega = f_o\frac{\partial}{\partial p}[\mathbf{V}_g\cdot\boldsymbol{\nabla}(\zeta_g + f)] - \nabla^2\left[\mathbf{V}_g\cdot\boldsymbol{\nabla}\left(\frac{\partial\phi}{\partial p}\right)\right], \qquad (1)$$

where $\nabla^2 = \partial^2/\partial x^2 + \partial^2/\partial y^2$, $\zeta_g = f_o^{-1}\nabla^2\phi$, and $\partial\phi/\partial p = -RT/p$. Traditionally, the forcing of vertical motions is diagnosed by considering the signs of the two terms on the rhs of (1). The first term represents the vertical derivative of horizontal geostrophic vorticity advection. The second term represents the Laplacian of horizontal temperature advection by the geostrophic wind. The existence of separate terms in (1) has led to the common attribution of quasigeostrophic (QG) vertical motions to ''upward increasing positive vorticity advection'' and/or ''warm-air advection'' as separate physical processes.

A convincing argument against such a practice was offered by Trenberth (1978). He carried out the derivatives on the rhs of (1) and found cancellation existed between the terms. He concluded that the rhs of (1) could be approximated by considering the advection of geostrophic absolute vorticity by the thermal wind. A similar result was achieved by Sutcliffe (1947) in his development theorem. Such simplification, however, was achieved at the expense of neglecting the so-called deformation term, which was suggested by both authors to be of minimal importance except in frontal regions.

Hoskins et al. (1978) introduced an alternative form of the QG omega equation in which the forcing for vertical motion is controlled by the divergence of the **Q** vector (specifically by $-2\boldsymbol{\nabla}\cdot\mathbf{Q}$). Note that **Q** is defined as

$$\mathbf{Q} = f\gamma\left[\left(-\frac{\partial\mathbf{V}_g}{\partial x}\cdot\boldsymbol{\nabla}\theta\right)\mathbf{i}, \left(-\frac{\partial\mathbf{V}_g}{\partial y}\cdot\boldsymbol{\nabla}\theta\right)\mathbf{j}\right], \qquad (2)$$

where $\gamma = (R/fp_o)(p_o/p)^{c_v/c_p}$ and is constant on isobaric surfaces. The divergence of **Q** contains all the forcing for QG vertical motions on the f plane, including the deformation term. However, it is not clear how the de-

Corresponding author address: Dr. Jonathan E. Martin, Atmospheric and Oceanic Sciences, University of Wisconsin—Madison, 1225 West Dayton Street, Madison, WI 53706-1695.
E-mail: jon@meteor.wisc.edu.

formation term is accounted for in the expression for $-2\nabla\cdot\mathbf{Q}$. Further, the $\mathbf{Q}$ vector is not as amenable to quick analysis as is the thermal wind advection of absolute vorticity. As a result, operational scientists might be inclined to use a form of the omega equation that does not contain the deformation term. The purpose of this note is to show the relationship between the deformation term in the Trenberth–Sutcliffe form of the omega equation and the alternative forcing expression, $-2\nabla\cdot\mathbf{Q}$. It will be shown that the deformation term represents half of the terms in that mathematical expression. Further, the relative magnitudes of the deformation and Trenberth–Sutcliffe forcings for QG omega at midtropospheric levels will be examined through a portion of the life cycle of a typical midlatitude cyclone.

2. The Trenberth–Sutcliffe forcing

Trenberth (1978) showed that, upon taking all the indicated derivatives, the rhs of (1) can be reduced to the following expression:

$$\text{rhs(1)} = J\left(\frac{\partial\phi}{\partial p}, \frac{2}{f}\nabla^2\phi + f\right) - \frac{2}{f}\Lambda\left(\phi, \frac{\partial\phi}{\partial p}\right), \quad (3)$$

where J is the Jacobian operator, equal to $J(A, B) = (\partial A/\partial x)(\partial B/\partial y) - (\partial A/\partial y)(\partial B/\partial x)$, and Λ is known as the deformation function (Wiin-Nielsen 1959) and is equal to

$$\Lambda(A, B) = -\frac{\partial^2 A}{\partial x\partial y}\left(\frac{\partial^2 B}{\partial x^2} - \frac{\partial^2 B}{\partial y^2}\right) + \frac{\partial^2 B}{\partial x\partial y}\left(\frac{\partial^2 A}{\partial x^2} - \frac{\partial^2 A}{\partial y^2}\right).$$

The first term in (3) is proportional to twice the advection of geostrophic relative vorticity by the thermal wind plus the advection of planetary vorticity by the meridional thermal wind. A nearly identical result was achieved by Sutcliffe (1947). The second term in (3) is the deformation term and it can be expanded into

$$-\frac{2}{f}\Lambda\left(\phi, \frac{\partial\phi}{\partial p}\right) = -\frac{2}{f}\left\{-\frac{\partial^2\phi}{\partial x\partial y}\left[\frac{\partial^2}{\partial x^2}\left(\frac{\partial\phi}{\partial p}\right) - \frac{\partial^2}{\partial y^2}\left(\frac{\partial\phi}{\partial p}\right)\right] + \frac{\partial^2}{\partial x\partial y}\left(\frac{\partial\phi}{\partial p}\right)\left(\frac{\partial^2\phi}{\partial x^2} - \frac{\partial^2\phi}{\partial y^2}\right)\right\}. \quad (4)$$

Since $\partial\phi/\partial p = -f\gamma\theta$, (4) can be rewritten as

$$-\frac{2}{f}\Lambda\left(\phi, \frac{\partial\phi}{\partial p}\right) = -2\gamma\left[-\frac{\partial^2\phi}{\partial x\partial y}\left(-\frac{\partial^2\theta}{\partial x^2} + \frac{\partial^2\theta}{\partial y^2}\right) - \frac{\partial^2\theta}{\partial x\partial y}\left(\frac{\partial^2\phi}{\partial x^2} - \frac{\partial^2\phi}{\partial y^2}\right)\right]. \quad (4a)$$

Substituting $f(\partial V_g/\partial x)$ and $-f(\partial U_g/\partial y)$ for $\partial^2\phi/\partial x^2$ and $\partial^2\phi/\partial y^2$, respectively, and noting that $\partial^2\phi/\partial x\partial y = -f(\partial U_g/\partial x) = f(\partial V_g/\partial y)$, (4a) can be rewritten as

$$-\frac{2}{f}\Lambda\left(\phi, \frac{\partial\phi}{\partial p}\right) = -2f\gamma\left(-\frac{\partial U_g}{\partial x}\frac{\partial^2\theta}{\partial x^2} - \frac{\partial V_g}{\partial y}\frac{\partial^2\theta}{\partial y^2} - \frac{\partial V_g}{\partial x}\frac{\partial^2\theta}{\partial x\partial y} - \frac{\partial U_g}{\partial y}\frac{\partial^2\theta}{\partial x\partial y}\right). \quad (5)$$

This equation can be expressed conveniently in the following form:

$$-\frac{2}{f}\Lambda\left(\phi, \frac{\partial\phi}{\partial p}\right) = -2f\gamma\left[-\frac{\partial\mathbf{V}_g}{\partial x}\cdot\boldsymbol{\nabla}\left(\frac{\partial\theta}{\partial x}\right) - \frac{\partial\mathbf{V}_g}{\partial y}\cdot\boldsymbol{\nabla}\left(\frac{\partial\theta}{\partial y}\right)\right], \quad (5a)$$

which is the form of the deformation term that facilitates its comparison with the forcing function of the $\mathbf{Q}$-vector form of the QG omega equation.

3. The Q-vector form of the QG omega equation

An alternative version of the QG omega equation on the f plane was given by Hoskins et al. (1978). In this formulation, the QG omega equation is written as

$$\left(\sigma\nabla^2 + f_o^2\frac{\partial^2}{\partial p^2}\right)\omega = -2\boldsymbol{\nabla}\cdot\mathbf{Q}, \quad (6)$$

where $\mathbf{Q}$ is given by

$$\mathbf{Q} = f\gamma\left[\left(-\frac{\partial\mathbf{V}_g}{\partial x}\cdot\boldsymbol{\nabla}\theta\right)\mathbf{i}, \left(-\frac{\partial\mathbf{V}_g}{\partial y}\cdot\boldsymbol{\nabla}\theta\right)\mathbf{j}\right].$$

Thus, the forcing of vertical motion is controlled by the divergence of the $\mathbf{Q}$ vector. It is instructive to evaluate the rhs of (6):

$$-2\boldsymbol{\nabla}\cdot\mathbf{Q} = -2\left(\frac{\partial}{\partial x}\mathbf{i} + \frac{\partial}{\partial y}\mathbf{j}\right) \cdot f\gamma\left[\left(-\frac{\partial\mathbf{V}_g}{\partial x}\cdot\boldsymbol{\nabla}\theta\right)\mathbf{i}, \left(-\frac{\partial\mathbf{V}_g}{\partial y}\cdot\boldsymbol{\nabla}\theta\right)\mathbf{j}\right]$$

or

$$-2\boldsymbol{\nabla}\cdot\mathbf{Q} = -2f\gamma\left[\frac{\partial}{\partial x}\left(-\frac{\partial\mathbf{V}_g}{\partial x}\cdot\boldsymbol{\nabla}\theta\right) + \frac{\partial}{\partial y}\left(-\frac{\partial\mathbf{V}_g}{\partial y}\cdot\boldsymbol{\nabla}\theta\right)\right]$$

$$= -2f\gamma\left\{\underbrace{\left[\frac{\partial}{\partial x}\left(-\frac{\partial\mathbf{V}_g}{\partial x}\right)\cdot\boldsymbol{\nabla}\theta + \frac{\partial}{\partial y}\left(-\frac{\partial\mathbf{V}_g}{\partial y}\right)\cdot\boldsymbol{\nabla}\theta\right]}_{\text{A}} + \underbrace{\left[-\frac{\partial\mathbf{V}_g}{\partial x}\cdot\boldsymbol{\nabla}\left(\frac{\partial\theta}{\partial x}\right) - \frac{\partial\mathbf{V}_g}{\partial y}\cdot\boldsymbol{\nabla}\left(\frac{\partial\theta}{\partial y}\right)\right]}_{\text{B}}\right\}. \quad (7)$$

Note that the right-hand side of (7) consists of two pairs of bracketed terms, labeled A and B. Pair A contains second derivatives of the geostrophic wind and first de-

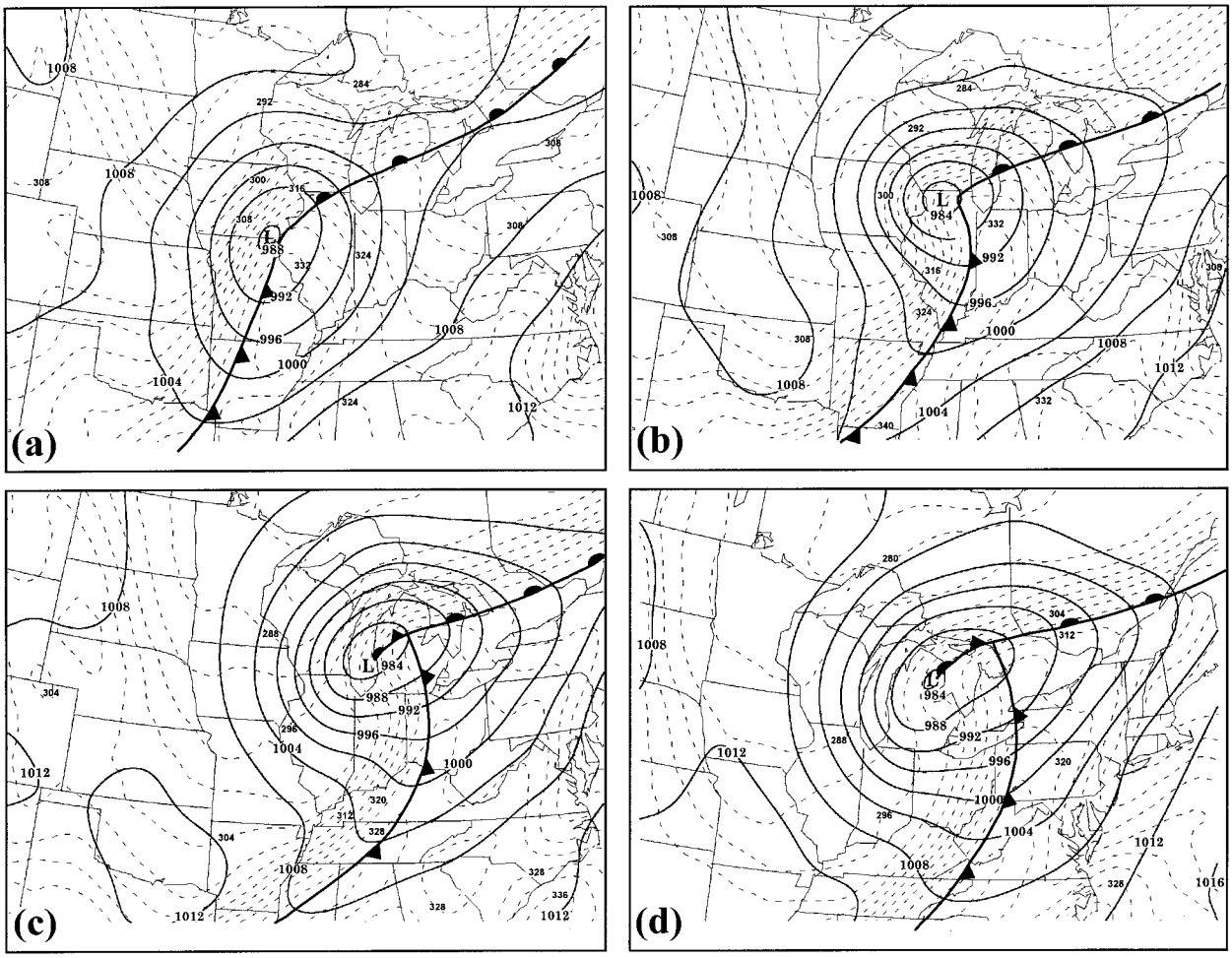

FIG. 1. (a) Six-hour forecast of sea level isobars and 1000-hPa equivalent potential temperature θ_e valid at 1800 UTC 30 April 1997 from the National Center for Environmental Prediction's Eta Model. Solid lines are isobars, labeled in hectopascals and contoured every 4 hPa. Dashed lines are contours of θ_e labeled in kelvins and contoured every 4 K. Surface frontal positions are indicated by conventional frontal symbols. (b) As for (a) except 12-h forecast valid at 0000 UTC 1 May 1997. (c) As for (a) except 18-h forecast valid at 0600 UTC 1 May 1997. (d) As for (a) except 24-h forecast valid at 1200 UTC 1 May 1997.

rivatives of θ and is equal to the advection of geostrophic relative vorticity by the thermal wind. Pair B contains second derivatives of θ and first derivatives of the geostrophic wind and is identically equal to the deformation term (5a). Thus, the deformation term represents half of the terms in the expression for $-2\nabla\cdot\mathbf{Q}$. The magnitude of the deformation term at midlevels throughout the evolution of a typical midlatitude cyclone will now be examined.

4. Magnitude of the deformation term

In work concerning the diagnosis of vertical motion, Wiin-Nielsen (1959) suggested that, given the fact that the isotherms tend to be parallel to the geopotential height lines in the middle troposphere, the deformation term will nearly vanish there. In fact, he directly calculated this term and found that it was, on average, less than one-half the mean value of $J[(\partial\phi/\partial p), (2f^{-1}\nabla^2\phi + f)]$ and that it occurred on a smaller scale than the Jacobian term. He was careful to note that these two statements were not generally true above or below 500 hPa, where the magnitude of the baroclinicity tends to be larger. Through calculations in several case studies, Trenberth (1978) found that the deformation term was generally negligible compared to the Jacobian term in the 400–600-hPa layer.

The following analysis examines the relative magnitudes of the Trenberth and deformation forcing terms at 600 hPa throughout a portion of the life cycle of a typical midlatitude cyclone. The 600-hPa level is shown as it is fairly representative of the entire 400–600-hPa layer. Isobaric levels well above and well below 600 hPa were examined during the course of this research and it was found that the deformation term was of considerable magnitude both near the lower-tropospheric frontal zones and near-isolated upper-tropospheric wind

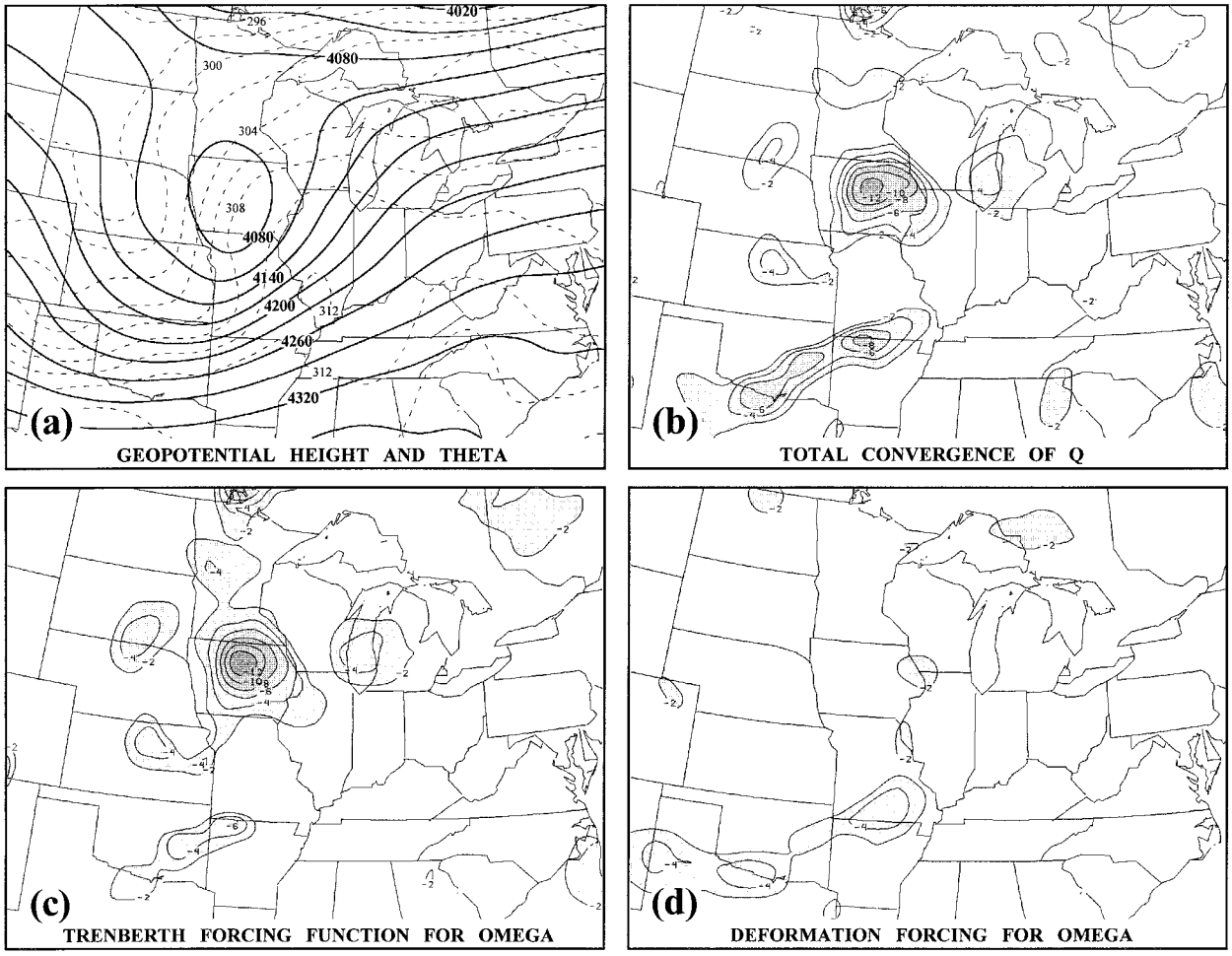

FIG. 2. (a) Six-hour forecast of geopotential height and temperature at 600 hPa valid at 1800 UTC 30 April 1997. Solid lines are geopotential heights labeled in meters and contoured every 30 m. Dashed lines are isotherms labeled in kelvins and contoured every 2 K. (b) Six-hour forecast, valid at 1800 UTC 30 April 1997, of 600-hPa convergence of the **Q** vector. Solid lines are **Q**-vector convergence labeled in 10^{-15} m^2 s^{-1} kg^{-1} and contoured every -2×10^{-15} m^2 s^{-1} kg^{-1} beginning at -2×10^{-15} m^2 s^{-1} kg^{-1}. Shading becomes darker as the values become more negative. (c) Six-hour forecast, valid at 1800 UTC 30 April 1997, of the advection of geostrophic vorticity by the thermal wind (Trenberth forcing, see text for explanation) evaluated at 600 hPa. Solid lines are Trenberth forcing labeled in -10^{-15} m^2 s^{-1} kg^{-1} and contoured every -2×10^{-15} m^2 s^{-1} kg^{-1} beginning at -2×10^{-15} m^2 s^{-1} kg^{-1}. Shading becomes darker as the values become more negative. (d) Six-hour forecast, valid at 1800 UTC 30 April 1997, of the deformation forcing of the QG omega equation at 600 hPa. Solid lines are contours of the deformation forcing labeled in -10^{-15} m^2 s^{-1} kg^{-1} and contoured every -2×10^{-15} m^2 s^{-1} kg^{-1} beginning at -2×10^{-15} m^2 s^{-1} kg^{-1}. Shading becomes darker as the values become more negative. All data come from the National Center for Environmental Prediction's Eta Model.

speed maxima in agreement with the findings of Wiin-Nielsen (1959).

In order to place the important midtropospheric analysis in a reasonable synoptic context, analyses of sea level pressure and surface frontal positions for the cyclone of interest, taken from an operational forecast by the National Center for Environmental Prediction's Eta Model, are shown in Fig. 1. At 1800 UTC 30 April 1997, the model surface cyclone was centered in northeast Missouri and had a sea level pressure minimum of 988 hPa (Fig. 1a). Clearly identifiable surface cold and warm fronts accompanied this cyclone. The cyclone was forecasted to move northeastward to a position near Chicago by 0000 UTC 1 May (Fig. 1b) and to deepen to 984 hPa. The initial stages of occlusion had begun by 0600 UTC 1 May as the model cyclone center moved only slightly eastward in the preceding 6 h and was centered over southeastern Lake Michigan at this time (Fig. 1c). A nascent surface occluded front was also evident. By 1200 UTC 1 May the surface cyclone was forecasted to be fully occluded and centered over northeastern lower Michigan with a sea level pressure minimum of 984 hPa (Fig. 1d).

The model forecast of 600-hPa geopotential and temperature valid at 1800 UTC 30 April are shown in Fig. 2a. A sharply curved shortwave trough axis was centered along the Missouri–Kansas border at this time with a geostrophic wind speed maximum located in south-

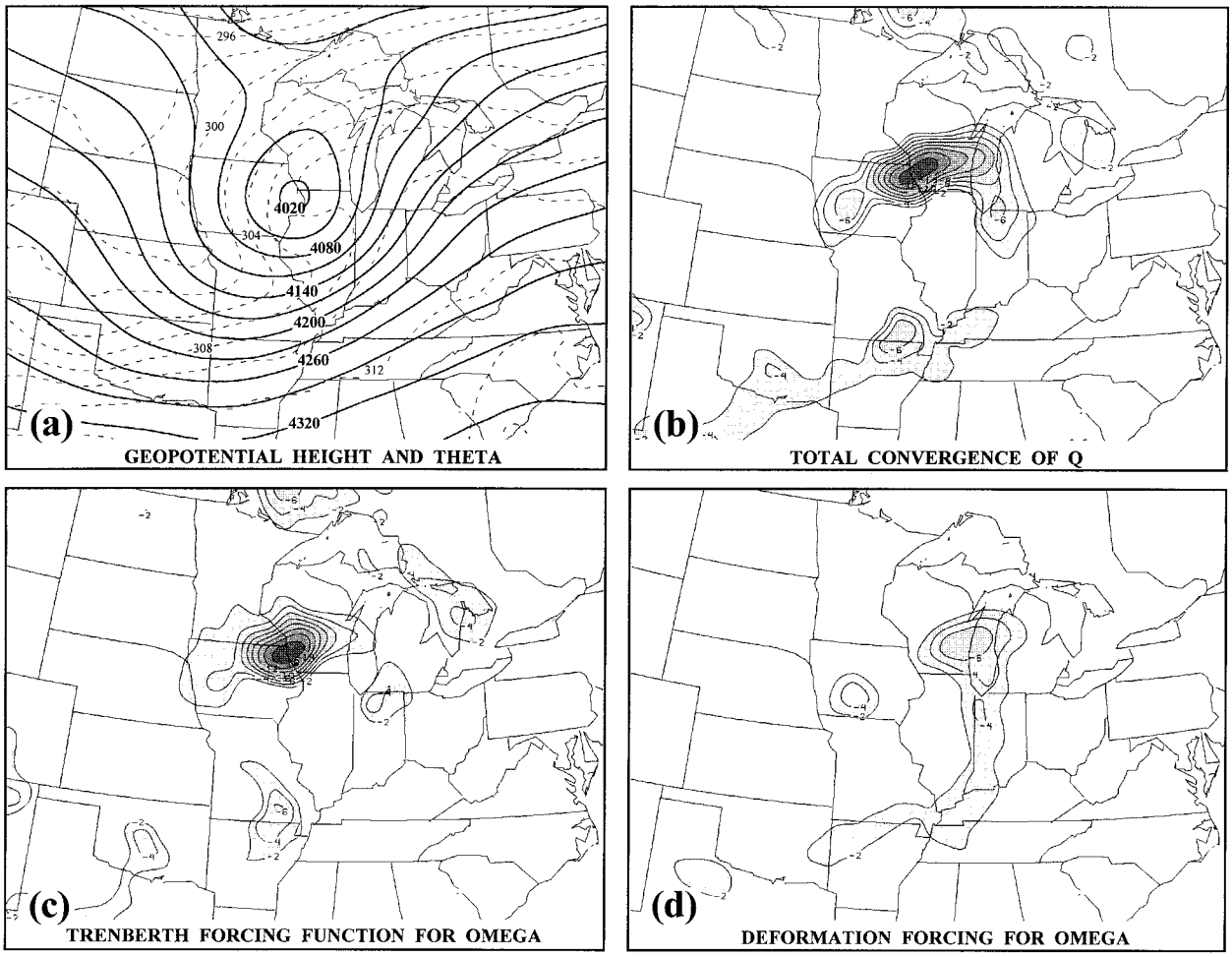

FIG. 3. (a) As for Fig. 2a except 12-h forecast valid at 0000 UTC 1 May 1997. (b) As for Fig. 2b except for 12-h forecast valid at 0000 UTC 1 May 1997. (c) As for Fig. 2c except for 12-h forecast valid at 0000 UTC 1 May 1997. (d) As for Fig. 2d except for 12-h forecast valid at 0000 UTC 1 May 1997.

central Missouri. Diffluent flow was superposed upon a temperature gradient in the lower Great Lakes states and a stronger southern baroclinic zone stretched from southwest Missouri across the panhandle of Texas.

The total convergence of **Q** at 600 hPa is shown in Fig. 2b. An isolated maxima existed in central Iowa along with a strip of **Q** convergence located roughly along the warm edge of the southern baroclinic zone. A comparison of Figs. 2b and 2c reveals that the **Q** convergence maximum in Iowa was nearly entirely accounted for by the advection of vorticity by the thermal wind (hereafter referred to as the ''Trenberth forcing'') (Fig. 2c). A portion of the strip of **Q** convergence associated with the southern baroclinic zone was also accounted for by this component of the forcing. Another portion of the southern forcing strip was accounted for by the deformation term (Fig. 2d), which resulted from the superposition of significant horizontal shear (i.e., large first derivative of $\mathbf{V}_g$) with the warm edge of the southern baroclinic zone (i.e., large second derivative of θ) in that region. It is clear, however, that the deformation term did not constitute a major midtropospheric forcing at this early stage in the cyclone life cycle.

By 0000 UTC 1 May, the model's forecast geopotential minimum at 600 hPa had deepened to 4020 m and was located over the Iowa–Illinois–Wisconsin border (Fig. 3a). The southern baroclinic zone identified previously stretched from near St. Louis, Missouri, to the panhandle of Texas in this forecast. The baroclinic zone in the lower Great Lakes states had tightened in response to strongly diffluent flow over northern Wisconsin and northeastern Minnesota.

Two regions of 600-hPa **Q** convergence were evident at this time. One was a semicircle-shaped region stretching from northern Indiana through southern Wisconsin into southwest Iowa (Fig. 3b). Very intense **Q** convergence characterized the center of this region. The second region was, as before, a strip of **Q** convergence aligned along the warm edge of the southern baroclinic zone in Arkansas, Oklahoma, and Texas. The western half of

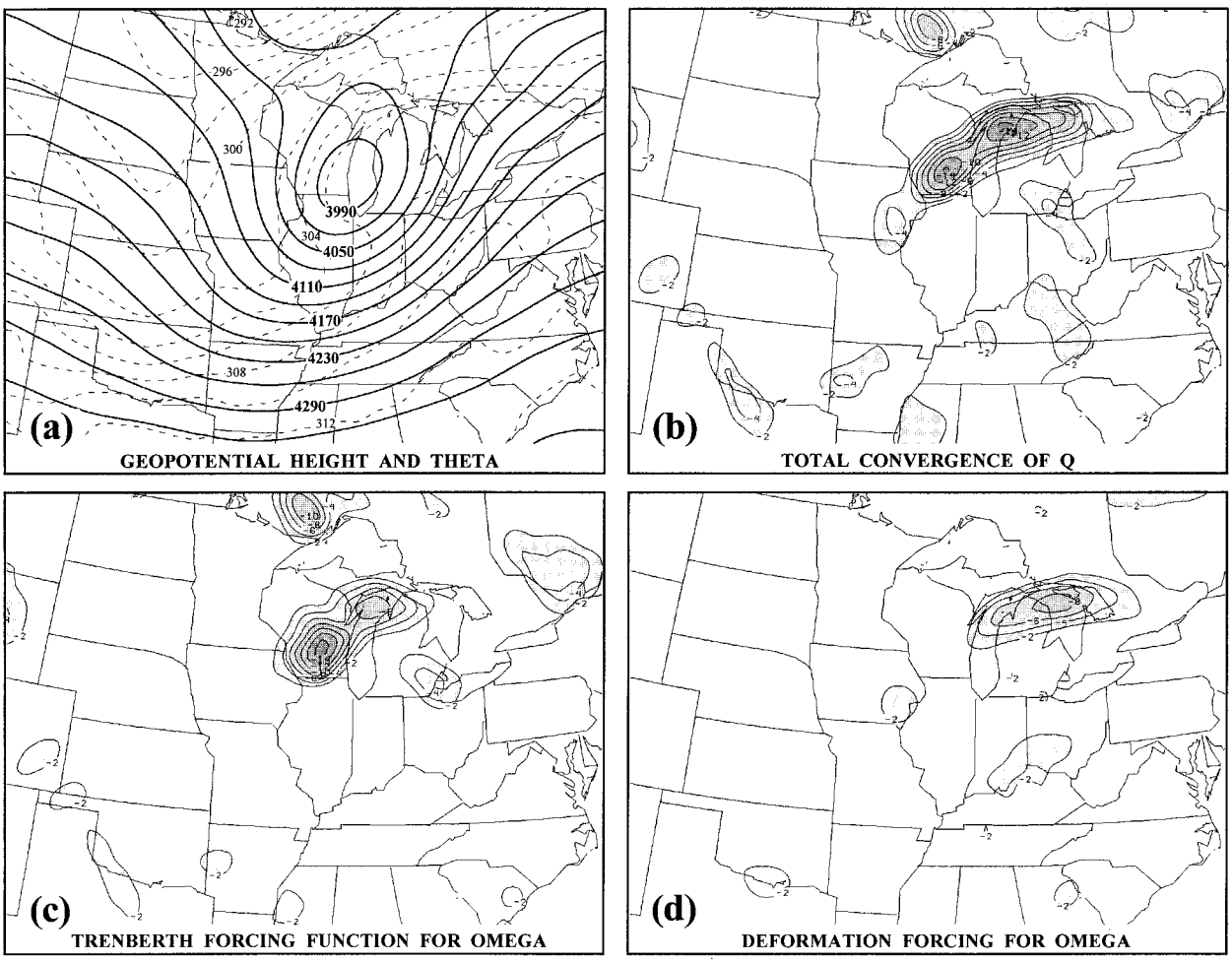

FIG. 4. (a) As for Fig. 2a except for 18-h forecast valid at 0600 UTC 1 May 1997. (b) As for Fig. 2b except for 18-h forecast valid at 0600 UTC 1 May 1997. (c) As for Fig. 2c except for 18-h forecast valid at 0600 UTC 1 May 1997. (d) As for Fig. 2d except for 18-h forecast valid at 0600 UTC 1 May 1997.

the more intense northern region of **Q** convergence was largely accounted for by the Trenberth forcing (Fig. 3c), as were the isolated regions of largest magnitude in the southern strip. The region of **Q** convergence over east-central Wisconsin, Lake Michigan, and northern Indiana was accounted for by the deformation term (Fig. 3d). Except for an axis that stretched from southeast Missouri to north Texas, the deformation forcing was located within fairly weak baroclinicity, but in a region characterized by horizontal shear and a large second derivative of θ. Also, the magnitude of the deformation forcing, though still less than half the magnitude of the largest Trenberth forcing, accounted for a significant portion of the total 600-hPa QG forcing for vertical motion associated with the cyclone at this time.

By 0600 UTC 1 May, a time at which the surface cyclone began to occlude (Fig. 1c), the model 600-hPa geopotential minimum had deepened modestly and migrated only slightly eastward to a position centered over Milwaukee, Wisconsin (Fig. 4a). A significant baroclinic zone stretched from southeast Iowa, through the upper peninsula of Michigan, into southeastern Ontario at 600 hPa.

The total **Q**-vector convergence at this time isolated a single major feature; an axis of large **Q** convergence stretching along the aforementioned baroclinic zone from southeast Iowa to the easternmost point of Lake Huron (Fig. 4b). Most of the western two-thirds of this strip was accounted for by the Trenberth forcing, which exhibited maxima over central Wisconsin and northern Lake Michigan at the time (Fig. 4c). The eastern extension of the total forcing over northern Lake Michigan and Lake Huron was accounted for by the significant deformation forcing at this time (Fig. 4d). This strong deformation forcing was coincident with an axis of maximum θ and geostrophic diffluence in the same region. Note that the magnitude of the deformation term at this time was larger than half the maximum value of the Trenberth forcing and that the areal extent of this forcing was comparable to that of the Trenberth forcing, testi-

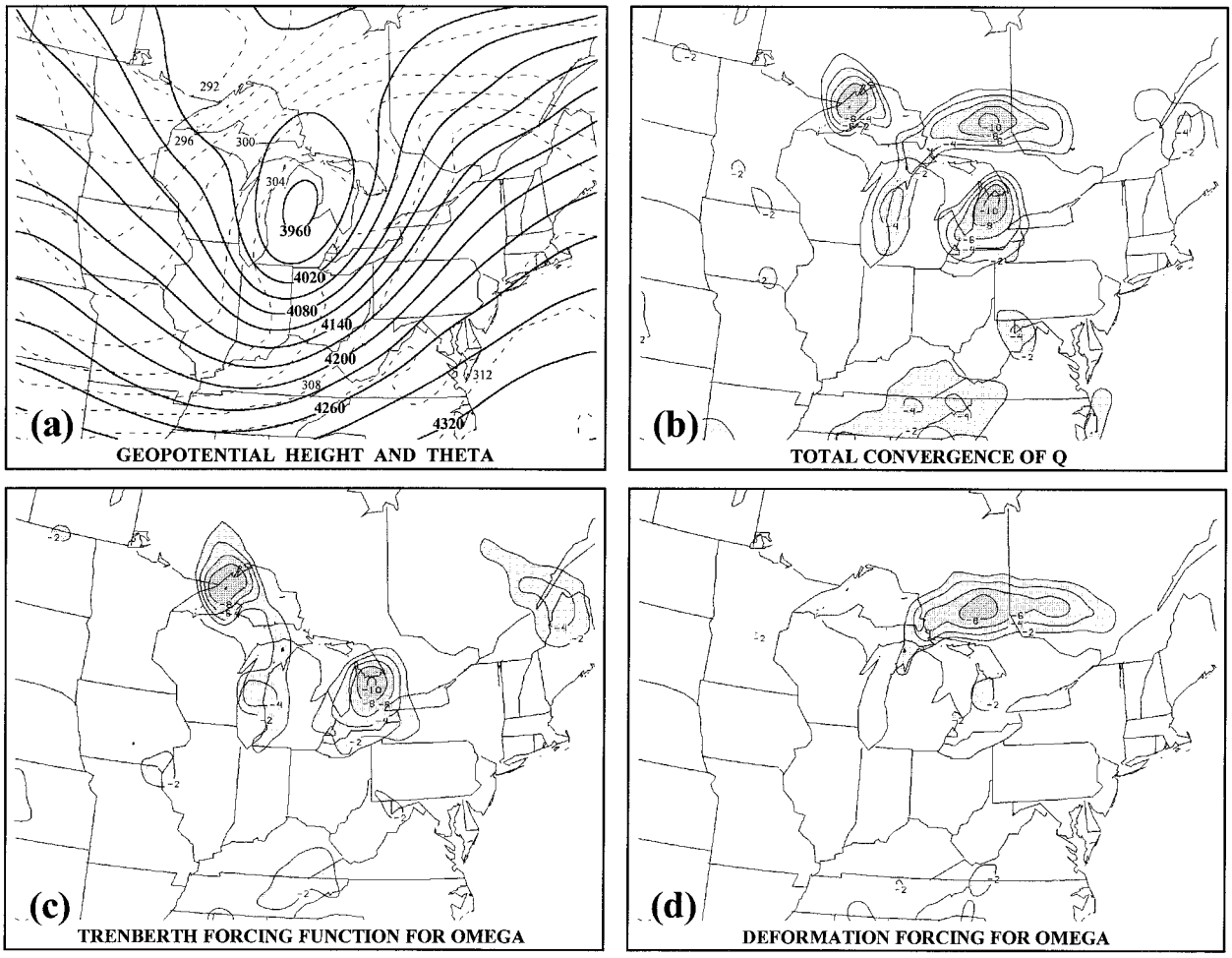

FIG. 5. (a) As for Fig. 2a except for 24-h forecast valid at 1200 UTC 1 May 1997. (b) As for Fig. 2b except for 24-h forecast valid at 1200 UTC 1 May 1997. (c) As for Fig. 2c except for 24-h forecast valid at 1200 UTC 1 May 1997. (d) As for Fig. 2d except for 24-h forecast valid at 1200 UTC 1 May 1997.

fying to the growing importance the midtropospheric deformation term appeared to have in the later stages of the cyclone life cycle.

At 1200 UTC 1 May the model cyclone was fully occluded. A hint of the thermal structure attendant with this occluded cyclone is evident in the 600-hPa geopotential height and temperature forecast at this time (Fig. 5a). The axis of maximum θ in southwestern Quebec, to the northeast of the geopotential minima, is a modest reflection of the more impressive warm occluded thermal structure exhibited by this storm in the lower troposphere (not shown).

The total **Q** convergence field at 600 hPa isolates three major features, all of which were located over the Great Lakes (Fig. 5b). Two isolated regions of **Q** convergence, one over central Lake Superior and another south of Lake Huron, straddled a significant axis of **Q** convergence that ran from southwestern Quebec, through southern Ontario, and along the eastern shore of Lake Michigan. The Trenberth forcing accounted for the two isolated maxima as well as a small portion of the axis of **Q** convergence (Fig. 5c). The most significant contribution to this axis, however, came from the deformation term (Fig. 5d). As was the case previously, the axis of maximum deformation forcing at this level was precisely collocated with the axis of maximum θ in the diffluent flow northeast of the geopotential minima at this time. It is interesting to note that at this fully occluded stage, the magnitude and areal coverage of the midtropospheric deformation forcing was comparable to the Trenberth forcing. Despite the fact that the thermal trough over Minnesota and Iowa in Fig. 5a was characterized by large second derivatives in θ, there was a distinct lack of deformation forcing associated with that feature (Fig. 5d). This fact highlights the necessity of *superposition* of horizontal variations in the geostrophic flow with thermal troughs and ridges in producing significant deformation forcing in the vicinity of such thermal features. The developing occluded quadrant of a cyclone is often characterized by a region of strong

horizontal geostrophic shear (or deformation) coincident with an amplifying thermal ridge. This circumstance is consistent with the observation, presented here, that the midtropospheric deformation forcing becomes increasingly more significant as the cyclone matures to the point of occlusion.

5. Conclusions

The forcing function of the QG omega equation on an f plane is represented completely in the divergence of the **Q** vector (Hoskins et al. 1978). Other approximations to this equation have simpler forms that are achieved at the expense of neglecting the so-called (Wiin-Nielsen 1959) deformation term, which is supposedly small except in lower-tropospheric frontal regions and near upper-tropospheric jet streaks. An alternative expression for the deformation term has been derived that illustrates its relationship to $-2\nabla\cdot\mathbf{Q}$, the forcing function in the **Q**-vector form of the quasi-geostrophic omega equation.

An analysis of the evolution of the midtropospheric (600 hPa) forcing of the QG omega equation throughout the life cycle of a typical midlatitude cyclone has been presented that both affirms prior work and suggest new insights. In agreement with prior conclusions (Wiin-Nielsen 1959; Trenberth 1978), the deformation forcing in the midtroposphere is less than half the magnitude of the Trenberth forcing during the development and early mature stages of the cyclone life cycle. The present case demonstrates, however, that the relative importance of the Trenberth and deformation forcings changes during the course of the cyclone life cycle as the midtropospheric deformation forcing gradually becomes comparable in magnitude and areal extent to the Trenberth forcing as the cyclone begins to occlude. Further, it appears that the midtropospheric deformation term is most significant in the occluded quadrant of the post–mature phase cyclone where a superposition occurs between the characteristic occluded thermal ridge and a region of large horizontal variation of the geostrophic flow.

The case illustrated here does not appear to be unique in any significant way from others that have been investigated in the course of this work. Thus, it may be that the deformation contribution to QG omega at midtropospheric levels generally acquires greater importance as a cyclone approaches and passes the occluded stage. The results presented here highlight the fact that neglect of the deformation term in the QG omega equation, always a risky proposition, is particularly inadvisable late in the cyclone life cycle.

Acknowledgments. The author wishes to thank Dr. Michael C. Morgan for his suggestion that the deformation term's relative magnitude may change during the cyclone life cycle and for other helpful comments. The insightful comments and suggestions of Dr. Juan Carlos Jusem were particularly helpful. Thanks also to Dr. John Young, Mr. Greg Postel, and Mr. Sebastien Korner for helpful comments and suggestions. This work was funded by the National Science Foundation under Grant ATM-9505849.

REFERENCES

Holton, J. R., 1992: *An Introduction to Dynamical Meteorology.* 3d ed. Academic Press, 511 pp.

Hoskins, B. J., I. Draghici, and H. C. Davies, 1978: A new look at the ω-equation. *Quart. J. Roy. Meteor. Soc.,* **104,** 31–38.

Sutcliffe, R. C., 1947: A contribution to the problem of development. *Quart. J. Roy. Meteor. Soc.,* **73,** 370–383.

Trenberth, K. E., 1978: On the interpretation of the diagnostic quasi-geostrophic omega equation. *Mon. Wea. Rev.,* **106,** 131–137.

Wiin-Nielsen, A., 1959: On a graphical method for an approximate determination of the vertical velocity in the mid-troposphere. *Tellus,* **11,** 432–440.